Nanotechnology **20** (2009) 495704 (7pp) doi:10.1088/0957-4484/20/49/495704

Stability and analysis of configuration-tunable bi-directional MWNT bearings

A Subramanian[1,2], **L X Dong**[1,3] **and B J Nelson**[1]

[1] Institute of Robotics and Intelligent Systems, Swiss Federal Institute of Technology (ETH) Zurich, CH-8092 Zurich, Switzerland
[2] Center for Integrated Nanotechnologies, Sandia National Laboratories, Albuquerque, NM 87185, USA
[3] Department of Electrical and Computer Engineering, Michigan State University, East Lansing, MI 48824, USA

E-mail: asubram@sandia.gov and bnelson@ethz.ch

Received 3 May 2009, in final form 21 October 2009
Published 11 November 2009
Online at stacks.iop.org/Nano/20/495704

Abstract
We report on the energetic and structural stability of configuration-tunable, bi-directional linear bearings based on cap-less, partial segments engineered within individual multi-walled carbon nanotubes (MWNTs). Using computational models, we show that an externally applied excitation force can be used to select an operating bearing configuration with a desired stiffness and operating frequency. Our models also demonstrate the possibility of simultaneous, independent operation of multiple bearings within a single NT segment, paving the way towards ultra-high device densities with molecular-scale footprints.

(Some figures in this article are in colour only in the electronic version)

1. Introduction

Nanomechanical elements that generate controllable motion at the molecular scale are essential building blocks for next-generation nanosystems such as nanomotors, switches, relays, resonators and sensors responding to diverse stimuli such as pressure, force and mass. One common approach towards creating nanoscale motion involves creating deformations within beams made of nanotubes (NTs) and nanowires (NWs) [1–6]. Previous reports have employed nanobeams in both cantilevered [1–3] and doubly clamped [4, 5] configurations (as in the conventional micro- and macro-world). Another mechanism that is unique to the nanoscale, and to multi-walled carbon nanotubes (MWNTs) in particular, involves inter-shell displacements within the nested shell MWNT architecture to create motion at the molecular scale. This mechanism has been exploited to realize both linear and rotary bearings with robust performance characteristics such as low friction, low wear and high repeatability [7–9]. Previous theoretical reports on nanobearings have studied the inter-shell interactions during nanomechanical motion with a specific focus on potential barriers and nature of motion [10–12]. These experimental and theoretical reports have shown that MWNT bearings possess a number of important advantages over NT/NW beams in terms of degrees of freedom (translational as well as rotational DOF possible), speed, size, power dissipation and displacement resolution down to the atomic scale.

2. Bi-directional nanobearings

Our investigation focuses on a novel bi-directional nanobearing architecture based on ultra-small, cap-less segments engineered within arc-grown MWNTs. In this nanobearing architecture (figure 1(a)), the outermost shell is fixed while the inner shells are free to slide axially in both directions within the outer housing. Typically, the anchoring of the outer shell is realized by depositing metal electrodes around the shell. One possible experimental embodiment that can be used to achieve this shell architecture is schematically illustrated in figure 1(b). In this image, an NT bridges five spatially separated electrodes while remaining flat and fully suspended in air in between the electrodes. Furthermore, the NT is broken at each of

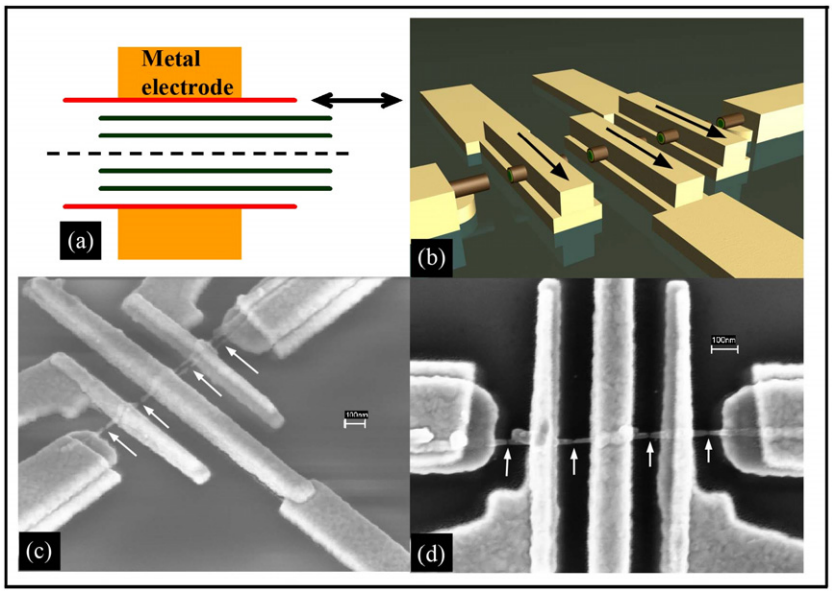

Figure 1. (a) The shell architecture of configuration-tunable bi-directional linear bearings based on partial, cap-less segments of an MWNT. The outermost shell, which remains anchored in place (typically using metallic electrodes), is shown in red while the inner shells that can displace axially are shown in dark green. The NT axis is shown in black dotted lines. (b) A cartoon illustrating one possible experimental embodiment of the shell architecture shown in panel (a). In this schematic, an MWNT bridges five electrodes after DEP nanoassembly. Post-assembly, the NT is etched via Joule heating to break it at the region between electrodes. The NT segments at the three inner electrodes (marked with arrows) have the geometry shown in panel (a). (c) SEM image (taken with a 40° stage tilt) of a fabricated nanostructure. This image shows two NTs assembled at a single location. (d) Top view of another nanostructure with configuration-tunable bearings. Arrows in panels (c) and (d) point to Joule heating induced to create bi-directional bearings.

the inter-electrode regions to create multiple, partial tubular segments from a single MWNT. The NT segments at the three inner electrodes (marked with arrows in figure 1(b)) possess an architecture that is highlighted in panel (a) and forms the focus of investigations within this report. To realize this construct, we first define metallic nanoelectrodes (15/45 nm Cr/Au) on silicon substrates with an insulating oxide layer using electron beam lithography and metal lift-off. Individual MWNTs are then assembled onto these electrodes using composite-field (AC + DC) dielectrophoresis [13, 14]. Next, a top layer of metallic contacts (also 15/45 nm Cr/Au) is defined using electron beam lithography and metal lift-off. This top metallic layer forms a conformal coating around the MWNT exterior and ensures that the outermost nanotube shell is anchored in place. Finally, a voltage above the NT breakdown threshold is applied between each pair of metallic electrodes to break the nanotube in the inter-electrode regions. Further details on this hybrid nanofabrication process can be found in [14, 15].

3. Structural and energetic stability

We developed computational models to provide new insights into the structural and energetic stability aspects of nanobearings with the architecture shown in figure 1. We show that these partial, cap-less segments of an individual MWNT function as configuration-tunable nanobearings that are differentiated in terms of the diameter and number of shells. This capability to reconfigure the geometry of the nanobearing after fabrication using a suitable external excitation signal provides a powerful tool to actively tune the structural stiffness and operating frequency of nanosystems.

A key aspect in which the structure presented in this effort differs from previous studies of bi-directional linear bearings [16–20] is summarized in figure 2. In earlier theoretical investigations, the NT core is assumed to have its cap intact at both ends. This results in a single sliding interface between the core and the fixed outer housing (figure 2(a)). In the structure presented in this paper, the NT core remains open at both ends and contains multiple core–shell sliding interfaces (figures 2(b)–(d)). This implies that multiple configurations with differences in the diameter and number of extruding shells are geometrically possible. In addition, more than one bearing can operate within a single NT segment (figure 2(d)), resulting in device densities that approach molecular-scale footprints. Though this results in increased device complexity, computational models indicate novel performance regimes with a potential for interesting applications. A detailed analysis of the inter-shell van der Waals interactions highlights the deterministic nature of this complex system and shows that a self-selecting mechanism based on the external excitation force determines the interface(s) at which shell sliding occurs. Another important aspect of this architecture is that it can be experimentally realized, as shown in figures 1(c) and (d). Other shell architectures previously reported in [16–20] (shown in figure 2(a)) are difficult to construct and have not been experimentally demonstrated to date. Within the extent of our knowledge, the only previous report on open-core MWNT bearings relates to the electrostatically actuated nanoswitches demonstrated in [21]. However, the key difference in our

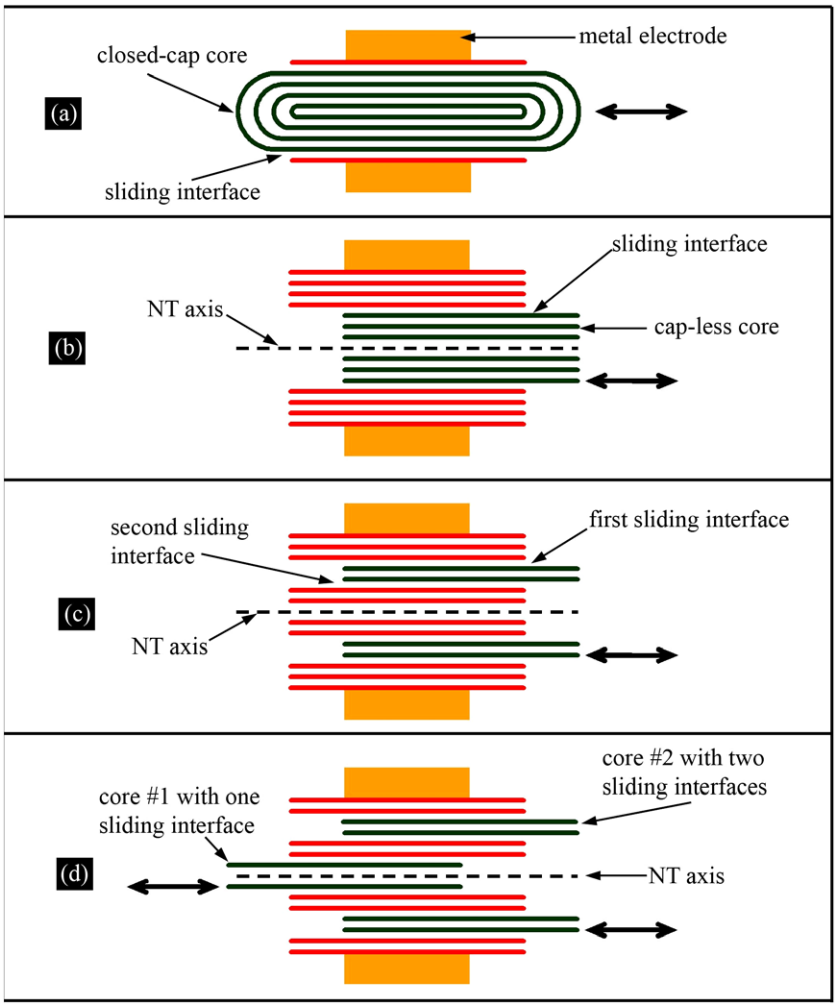

Figure 2. Bearing configurations where the stationary shells are shown in red while the moving core shells are shown in dark green. (a) Closed-cap core with a single sliding interface. This represents the geometry modeled in previous efforts. (b) Cap-less core with a single sliding interface. (c) A single-core configuration where some of the inner shells remain stationary. This results in a bearing with two sliding interfaces. (d) A two-core system where one core exhibits a single sliding interface while the second core translates across two interfaces.

architecture is that the core is cap-less at both ends as opposed to a single end in the previous report. A cap-less core on both sides enables bi-directional nanobearing operation. This cap-less geometry on both ends is a key requirement for realizing bearings with two sliding interfaces (figure 2(c)), and also for realizing a multiple-core system within a single NT segment (figure 2(d)). It is important to note that each of these operational modes cannot be realized using the unidirectional construct demonstrated in [21].

Our analysis of this cap-less, bi-directional bearing architecture is based on the modeling approach outlined in [16, 17] to compute the van der Waals interactions between individual NT shells. Specifically, our study pertains to the following aspects: (1) configurational stability of bearings with both single and double sliding interfaces, (2) van der Waals extrusion forces required for each of these energetically stable configurations and (3) the frequency spectrum of the energetically stable configurations. We employ an 11-shell MWNT with an outer diameter of 8 nm as a representative case study to present the findings of our investigation. These results are representative of multi-walled nanotubes, in general, and the analysis presented here can be used to determine stable configurations within any NT with a similar geometry.

Throughout this discussion, the numbering scheme employed starts from '1' at the innermost shell and increases progressively to the outermost shell. The Lennard-Jones potential that represents the interaction between an atom in shell 'i' and another atom in shell 'j' is given by

$$\phi = \frac{C_{12}}{s^{12}} - \frac{C_6}{s^6} \tag{1}$$

where C_6 and C_{12} represent the attractive and repulsive components of the interatomic forces, respectively. In the above expression, s denotes the spacing between the two atoms. The interaction between an atom in shell i and all the atoms in shell j can then be computed by using a pair-wise summation between the individual atoms. An alternative solution to this problem has been outlined in [16, 17] and involves using a continuum distribution for the atoms on the surface of shell j (with a density $4\sqrt{3}/9a^2$). We have employed this technique based on the continuum approximation developed in [17], in which the van der Waals

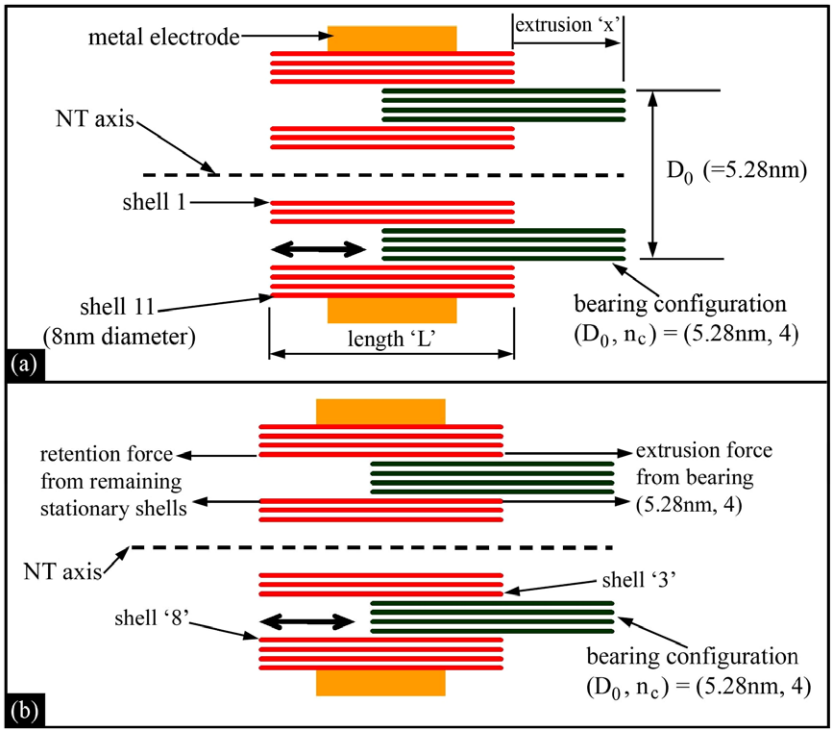

Figure 3. (a) The image illustrates an 11-shell MWNT with a single-core bearing. The notation used to identify the bearing configuration and its extrusion is illustrated schematically in this figure. (b) Energetic stability considerations for nanobearing (5.28 nm, 4). As indicated, shells 3 and 8 are the nearest stationary neighbors at the sliding interfaces of this bearing. The competing extrusion and retention force components are highlighted in this image.

interaction between an atom in shell i and all the atoms within shell j (with $i < j$) is given by

$$\Phi_{i,j} = \frac{A\sqrt{3}\pi}{9a^2}\left[21d_0^6 I_{11}(g) - 64I_5(g)\right](r+g) \qquad (2)$$

where A (=24.3 × 10^{-79} J m^6), d_0 (=2.7), r and g (=$(j-i)d_0$) represent the energy constant, interatomic distance, radius of shell i and spacing between shells i and j, respectively. In the above expression, A, d_0, r and g are normalized with respect to a (=0.142 nm), which represents the carbon–carbon bond length. In (2), $I_{11}(g)$ and $I_5(g)$ are elliptical integrals defined by

$$I_m(g) = (2r+g)^{-m}\int_0^{\pi/2}[1 - K(g)\cos^2\theta]^{-m/2}\,\mathrm{d}\theta \qquad (3)$$

where $K(g) = \frac{4(r+g)r}{(2r+g)^2}$. The van der Waals interaction energy between all atoms on interior shell i and exterior shell j can then be computed as

$$E_{\mathrm{vdw}}(i,j) = \frac{4\sqrt{3}\pi Dl}{9a^2}\Phi_{i,j} \qquad (4)$$

where D represents the diameter of shell i, while l represents the length of overlap between the two shells under consideration. We would also like to highlight the fact that this assumption of a continuum distribution of carbon atoms on the nanotube shells has been shown to be a valid approximation for NTs with diameters larger than 0.3 nm (which holds true in our case). Calculations in [17] have shown that this approximation varies from a discrete atomic distribution calculation (which explicitly takes into account NT chirality) by less than 3% for NTs with diameters greater than 0.3 nm.

Equation (2), which represents the interaction between any two shells, can be extended to compute the net van der Waals interaction experienced by a multiple-shell core that is extruded with respect to the remaining NT shells. The configuration of such a multiple-shell nanobearing is denoted by the notation (D_0, n_c), where D_0 represents the outer diameter of the moving core and n_c represents the number of core shells. The number of stationary shells that are located inside and outside of the moving core are denoted by $n_{s,\mathrm{int}}$ and $n_{s,\mathrm{ext}}$, respectively. This notation for describing the sliding interfaces and the resulting bearing configuration is shown in figure 3(a) for the 11-shell NT under consideration. The net van der Waals interaction energy experienced by the moving core can be obtained by a pair-wise summation of the interactions between constituent shells. For a bearing with configuration (D_0, n_c) that is extruded by a distance x, the energy stored in the core due to interactions with the inner stationary shells can be expressed as

$$E_{\mathrm{vdw,int}}(D_0, n_c) = \frac{4\sqrt{3}\pi(L-x)}{9a^2}\sum_{i=1}^{n_{s,\mathrm{int}}} D_i\left(\sum_{j=1}^{n_c}\Phi_{i,j}\right) \qquad (5)$$

where D_i represents the diameter of shell i. In addition, L denotes the length of shells while x represents the distance by which the core is extruded. Similarly, the energy stored in the

core due to interactions with the outer stationary shells is given by

$$E_{\mathrm{vdw,ext}}(D_0, n_c) = \frac{4\sqrt{3}\pi(L-x)}{9a^2}\sum_{i=1}^{n_c} D_i\left(\sum_{j=1}^{n_{s,\mathrm{ext}}}\Phi_{i,j}\right). \quad (6)$$

The total van der Waals energy stored in the core can then be written as

$$E_{\mathrm{vdw}}(D_0, n_c) = E_{\mathrm{vdw,int}}(D_0, n_c) + E_{\mathrm{vdw,ext}}(D_0, n_c). \quad (7)$$

From (5)–(7), the restoring force experienced by the core can be computed as

$$F_{\mathrm{vdw}}(D_0, n_c) = \frac{\mathrm{d}E_{\mathrm{vdw}}(D_0, n_c)}{\mathrm{d}x} = \frac{4\sqrt{3}\pi}{9a^2}\left[\sum_{i=1}^{n_{s,\mathrm{int}}} D_i\left(\sum_{j=1}^{n_c}\Phi_{i,j}\right) + \sum_{i=1}^{n_c} D_i\left(\sum_{j=1}^{n_{s,\mathrm{ext}}}\Phi_{i,j}\right)\right]. \quad (8)$$

From the above expression, it is evident that the van der Waals restoring force is independent of the extrusion distance and remains constant for a given nanobearing configuration.

The most significant conclusion that emerges from the analysis of these open-capped structures is that, for a given NT (in terms of the number of shells and outer diameter), there exist only a finite number of configurations that are energetically stable. This is best explained by a representative nanobearing example involving the 11-shell NT under consideration (shown in figure 3(b)). For a nanobearing with configuration (5.28 nm, 4), shells 3 and 8 form its nearest neighbors at the two sliding interfaces (the numbering scheme starts from 1 at the innermost NT shell and progressively increases to 11 at the outermost). Each of these nearest neighbors experience competing force components. For instance, shell 3 experiences an extrusion force due to the motion of shells 4–7. At the same time, van der Waals interactions with the remaining stationary NT layers result in a force component on shell 3 that opposes this extrusion force. The relative magnitudes of these two opposing components eventually determines whether shell 3 remains stationary or tends to extrude along with shells 4–7. The behavior of shell 8 is also similarly dictated by these two competing retention and extrusion force components. As a result, the nanobearing (5.28 nm, 4) is inherently stable only if shells 3 and 8 are both stationary. Otherwise, an externally applied restraining force, which acts locally on shells 3 and 8, would be required to attain this configuration.

A computational code was developed to calculate the extrusion/retention force components and determine the energetically stable core configurations for a given NT. The results from these numerical computations are highlighted in figure 4(a). In this 3D plot, the z axis represents the configurational stability index, which assumes a value of 1 for a stable configuration. A value of 0 implies that the configuration is either energetically unfavorable or geometrically infeasible. From this plot, it is evident that there are 12 distinct, single-core nanobearing configurations that can be realized within an open-capped MWNT with 11 shells and an outer diameter of 8 nm. In addition, the external excitation forces that

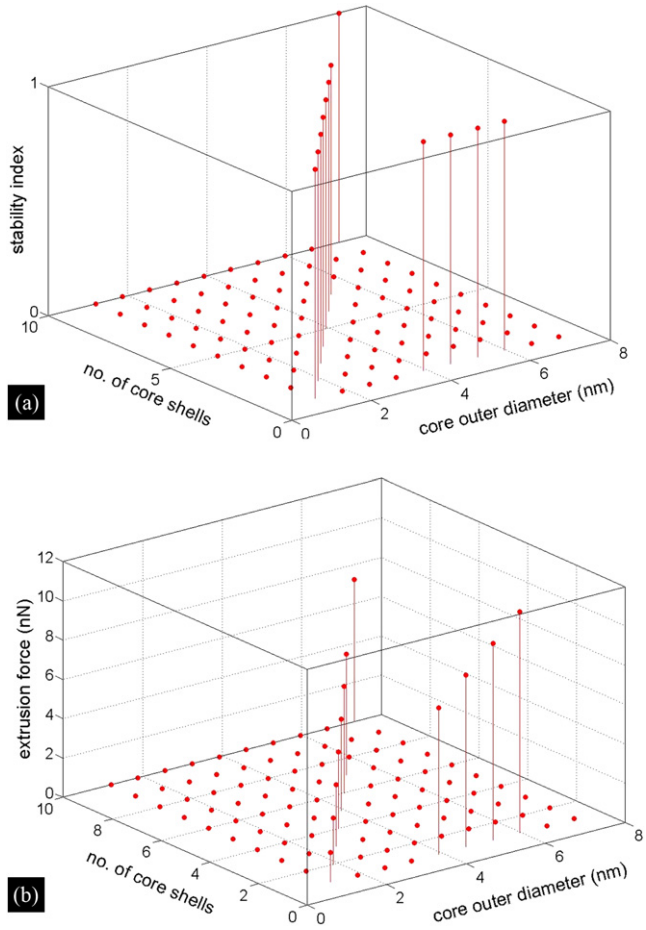

Figure 4. Configurational stability analysis for an 11-shell NT with an outer diameter of 8 nm. (a) 3D plot of the stability index (1 = stable and 0 = unstable) as a function of core outer diameter and number of shells. (b) The external extrusion force required to displace the core in each of the stable configurations.

are required to extrude each of these stable nanobearings are shown in panel (b).

The results illustrated in figure 4 are also summarized in table 1 for the stable nanobearing configurations. A careful analysis of this tabulated data highlights several unique and interesting aspects of these bi-directional mechanisms. It can be seen that, depending on the magnitude and location of the external excitation force, the precise shells that extrude are based on a self-selection mechanism. For instance, when the extrusion force is 7.5 nN there are several possible bearing configurations, depending on the location where this force is applied. If the force is applied locally to shell 1, then just this shell will extrude. However, if this force is distributed uniformly over shells 1 to n (where n is less than 10), then the innermost n shells will extrude. Thus, it is possible to realize an excitation-based, tunable nanobearing from these structures. This characteristic of MWNTs has not been previously reported.

Another aspect that emerges from these computations is that, though single-shell bearings are energetically stable, the extrusion forces required to actuate these bearings are higher than those required for multiple-shell bearings. This

Table 1. Summary of energetically stable nanobearing configurations for an MWNT with 11 shells and an outer diameter of 8 nm.

Bearing configuration	Extrusion force (nN)	Resonant frequency (GHz)
(1.2 nm, 1)	1.50	3.79
(1.88 nm, 2)	2.37	2.97
(2.56 nm, 3)	3.15	2.53
(3.24 nm, 4)	3.91	2.25
(3.92 nm, 5)	4.67	2.04
(4.6 nm, 6)	5.42	1.89
(5.28 nm, 7)	6.15	1.76
(7.32 nm, 10)	7.22	1.39
(3.92 nm, 1)	7.43	4.88
(4.6 nm, 1)	8.73	4.84
(5.28 nm, 1)	10.00	4.82
(5.96 nm, 1)	11.26	4.79

is attributed to the higher number of shells that exert restoring van der Waals forces in the case of single-shell bearings. The extrusion forces for bearing operation are estimated to be in the nN regime and are within the range of values experimentally measured for telescoping nanotubes [7, 8].

Another interesting aspect of these constructs is that each bearing configuration has a distinct natural frequency. The resonant frequency of these structures in the interlayer sliding mode can be estimated using the following expression [16, 17]:

$$f = \frac{1}{4}\sqrt{\frac{F_{\mathrm{vdw}}(D_0, n_c)}{2\Delta M}} \tag{9}$$

where $F_{\mathrm{vdw}}(D_0, n_c)$ is the van der Waals retraction force defined in (8). In addition, Δ and M represent the initial extrusion and mass of the core, respectively. The resonant frequencies of the stable nanobearing configurations were computed using (9) for the 11-shell, 8 nm outer diameter NT under consideration. An initial extrusion of 5 nm was assumed in these computations. The experimentally observed inter-segment spacing is of the order of 6–15 nm, and the assumption of a 5 nm initial extrusion is consistent with this geometry. The results from frequency computations using (9) are also summarized in table 1. From these results, it is evident that the oscillation frequency of these structures varies between 1.39 and 4.88 GHz for nanobearing configurations that can be realized using the NT under consideration. In addition, the resonant frequencies are found to be higher for single-core bearings as compared to the multiple-core structures. This is to be expected due to the higher retraction forces as well as lower mass associated with the single-shell mechanisms.

Finally, the simultaneous and independent operation of multiple cores within a single NT segment as shown in figure 2(d) can be considered in this analysis. In the case of the 11-shell NT presented above, there are no energetically stable multiple-core configurations. For instance, when the (1.2 nm, 1) and (5.96 nm, 1) bearings extrude simultaneously in the same direction, then the intermediate shells (numbered 2–7) experience extrusion force components from both the bearings that reinforce each other, and our computations show that these will not stay stationary. Thus, it is not possible to have (1.2 nm, 1) and (5.96 nm, 1) bearings operating simultaneously within a 11-shell MWNT. However, these multiple bearing configurations become viable mechanisms within larger diameter NTs when the extruding cores are separated by a sufficient number of intermediate shells. For instance, in a 21-shell MWNT with an outer diameter of 14.8 nm, bearings with (1.2 nm, 1) and (10.04 nm, 1) configurations can be independently operated at the same time. This capability to realize multiple, independent bearings within a single NT segment represents a powerful tool for realizing higher device densities that approach molecular footprints. Also, unlike the closed-cap bearings theoretically discussed in [16–20], this capability is unique to the cap-less architecture fabricated and discussed here.

4. Conclusions

We have presented a comprehensive overview of the energetic and structural stability aspects of a novel, open-cap bi-directional bearing architecture constructed within individual MWNTs. Computational models have been employed to analyze the van der Waals interactions between the individual NT shells. These models provide new insights into configurational stability, retraction forces and oscillation frequencies of these structures. These results illustrate the suitability of these structures for unique molecular machines where the structural stiffness and operational frequencies are tuned by varying the magnitude and profile of externally applied excitation forces. In addition, the models point to the possibility of operating multiple, independent bearings within individual MWNT segments, leading to ultra-large device densities that approach molecular-scale footprints.

References

[1] Ke C H and Espinosa H D 2006 *Small* **2** 1484
[2] Lee S W, Lee D S, Morjan R E, Jhang S H, Sveningsson M, Nerushev O A, Park Y W and Campbell E E B 2004 *Nano Lett.* **4** 2027
[3] Jang J E, Cha S N, Choi Y, Amaratunga G A J, Kang D J, Hasko D G, Jung J E and Kim J M 2005 *Appl. Phys. Lett.* **87** 163114
[4] Kaul A B, Wong E W, Epp L and Hunt B D 2006 *Nano Lett.* **6** 942
[5] Dujardin E, Derycke V, Goffman M F, Lefevre R and Bourgoin J P 2005 *Appl. Phys. Lett.* **87** 193107
[6] Kinaret J M, Nord T and Viefers S 2003 *Appl. Phys. Lett.* **82** 1287
[7] Cumings J and Zettl A 2000 *Science* **289** 602
[8] Kis A, Jensen K, Aloni S, Mickelson W and Zettl A 2006 *Phys. Rev. Lett.* **97** 025501
[9] Fennimore A M, Yuzvinsky T D, Han W Q, Fuhrer M S, Cumings J and Zettl A 2003 *Nature* **424** 408
[10] Saito R, Matsuo R, Kimura T, Dresselhaus G and Dresselhaus M S 2001 *Chem. Phys. Lett.* **348** 187
[11] Belikov A V, Lozovik Y E, Nikolaev A G and Popov A M 2004 *Chem. Phys. Lett.* **385** 72
[12] Shen G A, Namilae S and Chandra N 2006 *Mater. Sci. Eng.* A **429** 66
[13] Chung J Y, Lee K H, Lee J H and Ruoff R S 2004 *Langmuir* **20** 3011
[14] Subramanian A, Vikramaditya B, Dong L X, Bell D J and Nelson B J 2005 *Robotics: Science and Systems I* ed S Thrun *et al* (Cambridge, MA: MIT Press) p 327

[15] Subramanian A, Dong L X, Tharian J, Sennhauser U and Nelson B J 2007 *Nanotechnology* **18** 075703
[16] Zheng Q S and Jiang Q 2002 *Phys. Rev. Lett.* **88** 045503
[17] Zheng Q S, Liu J Z and Jiang Q 2002 *Phys. Rev.* B **65** 245409
[18] Guo W L, Guo Y F, Gao H J, Zheng Q S and Zhong W Y 2003 *Phys. Rev. Lett.* **91** 125501
[19] Rivera J L, McCabe C and Cummings P T 2003 *Nano Lett.* **3** 1001
[20] Legoas S B, Coluci V R, Braga S F, Coura P Z, Dantas S O and Galvao D S 2003 *Phys. Rev. Lett.* **90** 055504
[21] Deshpande V V, Chiu H Y, Postma H W Ch, Miko C, Forro L and Bockrath M 2006 *Nano Lett.* **6** 1092